HHS Public Access

Author manuscript

Arterioscler Thromb Vasc Biol. Author manuscript; available in PMC 2021 July 01.

Published in final edited form as:

Arterioscler Thromb Vasc Biol. 2020 July ; 40(7): 1680–1694. doi:10.1161/ATVBAHA.119.313765.

DYSREGULATION OF FOXO1 DRIVES CALCIFICATION IN ACDC (ARTERIAL CALCIFICATION DUE TO DEFICIENCY OF CD73) AND IS PRESENT IN PERIPHERAL ARTERY DISEASE

William J. Moorhead III[1,2,*], **Claire C. Chu**[1,2,*], **Rolando A. Cuevas**[1,2], **Jack Callahan IV**[1,2], **Ryan Wong**[1,2], **Cailyn Regan**[1,2], **Camille K. Boufford**[1,2], **Swastika Sur**[1,2], **Mingjun Liu**[1,2], **Delphine Gomez**[1,2], **Jason N. MacTaggart**[4], **Alexey Kamenskiy**[5], **Manfred Boehm**[6], **Cynthia St. Hilaire**[1,2,3]

[1]Department of Medicine, Division of Cardiology, University of Pittsburgh, Pittsburgh, PA, USA

[2]Pittsburgh Heart, Lung, and Blood Vascular Medicine Institute, University of Pittsburgh, Pittsburgh, PA, USA

[3]Department of Bioengineering, Swanson School of Engineering, University of Pittsburgh, Pittsburgh, PA, USA

[4]Department of Surgery, University of Nebraska Medical Center, Omaha, NE, USA

[5]Department of Biomechanics, University of Nebraska Omaha, Omaha, NE, USA

[6]Laboratory of Cardiovascular Regenerative Medicine, National Heart, Lung, and Blood Institute, Bethesda, MD, USA.

Abstract

OBJECTIVE: The recessive disease Arterial Calcification due to Deficiency of CD73 (ACDC) presents with extensive non-atherosclerotic medial layer calcification in lower extremity arteries. Lack of CD73 induces a concomitant increase in tissue non-specific alkaline phosphatase (*ALPL*/TNAP), a key enzyme in ectopic mineralization. Our aim was to investigate how loss of CD73 activity leads to increased *ALPL* expression and calcification in CD73-deficient patients and assess whether this mechanism may apply to peripheral artery disease calcification.

APPROACH AND RESULTS: We previously developed a patient-specific disease model using ACDC primary dermal fibroblasts that recapitulates the calcification phenotype in vitro. We found that lack of CD73-mediated adenosine signaling reduced cAMP production and resulted in increased activation of AKT. The AKT/mTOR axis blocks autophagy and inducing autophagy prevented calcification, however we did not observe autophagy defects in ACDC cells. In silico analysis identified a putative FOXO1 binding site in the human *ALPL* promoter. Exogenous AMP induced FOXO1 nuclear localization in ACDC but not in control cells, and this was prevented with a cAMP analogue or activation of A2a/2b adenosine receptors. Inhibiting FOXO1 reduced *ALPL*

Corresponding Author Contact Info: Cynthia St. Hilaire, PhD, University of Pittsburgh, BSTWR 1744.1, 200 Lothrop Street, Pittsburgh, PA 15261, 412.648.9441 sthilair@pitt.edu.

*denotes equal contribution

DISCLOSURES

None

expression and TNAP activity and prevented calcification. Mutating the FOXO1 binding site reduced *ALPL* promoter activation. Importantly, we provide evidence that non-ACDC calcified femoropopliteal arteries exhibit decreased CD73 and increased FOXO1 levels compared to control arteries.

CONCLUSIONS: These data show that lack of CD73-mediated cAMP signaling promotes expression of the human *ALPL* gene via a FOXO1-dependent mechanism. Decreased CD73 and increased FOXO1 was also observed in more common peripheral artery disease calcification.

GRAPHICAL ABSTRACT:

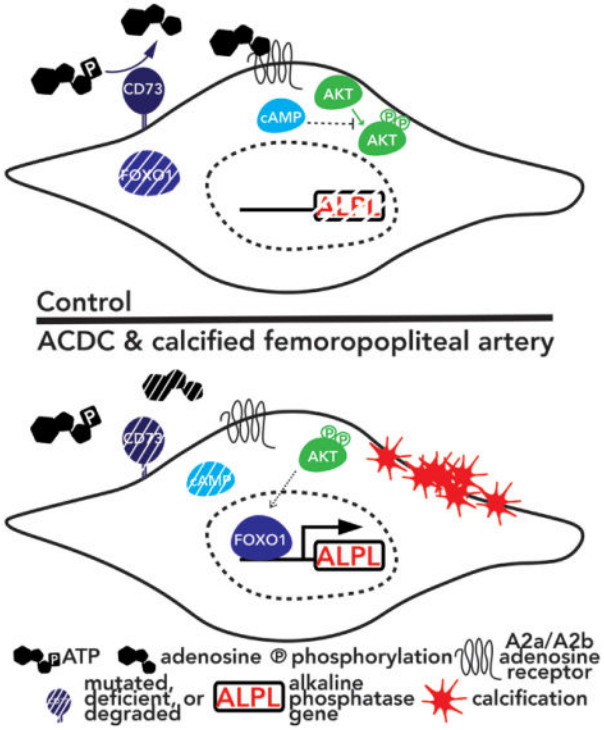

Dysregulation of FOXO1 signaling drives calcification in ACDC and is present in peripheral artery disease

Keywords

vascular calcification; alkaline phosphatase; CD73; FOXO1; femoropopliteal artery

INTRODUCTION

Vascular calcification is an active process found in a variety of disease states. Luminal calcification is present in atherosclerotic plaques where it strongly correlates with an increased risk of coronary events.[1] Medial layer calcification is a co-morbidity and complication of prolonged diseases such as chronic kidney disease, diabetes, rheumatoid arthritis, and aging. In contrast to plaque calcification, medial calcification is often found along the elastic lamina and in areas surrounding smooth muscle cells.[2] Currently no therapy has been developed that is able to prevent, halt, or reverse ectopic calcification in the

vasculature.[3] To date, two genetic diseases have been identified in which mutations induce de novo calcifications in the medial layer of large elastic and smaller muscular arteries – Generalized Arterial Calcification of Infancy (GACI, OMIM # 208000) and Arterial Calcification due to Deficiency of CD73 (ACDC, OMIM # 211800).[4, 5] GACI and ACDC are rare autosomal recessive diseases caused by inactivating mutations in *ENPP1* and *NT5E* (encoding for CD73 protein), respectively. ENPP1 and CD73 are extracellular enzymes that function as key components in the breakdown of extracellular nucleosides: ATP is metabolized to AMP and pyrophosphate by ENPP1, and CD73 converts AMP into adenosine and inorganic phosphate.[6] The stresses thought to contribute to medial calcification, such as mechanical stress and inflammation, are the same stresses known to modulate ATP release and subsequent adenosine production.[7–9]

The CD73-deficient mouse does not recapitulate the vascular phenotypes seen in CD73-deficient patients with ACDC, thus this murine model is an ineffective tool to study the mechanisms driving the vascular phenotypes in ACDC pathogenesis and disease progression.[10–12] We previously developed an in vivo disease model utilizing CD73-deficient induced pluripotent stem cells (iPSCs) and found accelerated calcification in CD73-deficient iPSC teratomas while control iPSC teratomas exhibited no such phenotype.[13] CD73-deficient iPSC-derived mesenchymal stem cells more readily differentiated down the osteogenic lineage and increased expression and activity of tissue non-specific alkaline phosphatase (*ALPL*/TNAP). While TNAP is a marker for stem cells, it is also a key enzyme in ectopic mineralization as it preferentially breaks down the endogenous mineralization inhibitor, pyrophosphate, into inorganic phosphate, a building block necessary for calcification.[14] We found that reduced adenosine signaling due to CD73 mutations caused cells to upregulate *ALPL* gene expression, and that the TNAP enzyme can somewhat compensate for CD73 deficiency by hydrolyzing AMP to adenosine, but with 100-fold less efficiency.[13] These observations confirm that CD73-mediated adenosine signaling is a critical component to vascular homeostasis.

While it is evident that TNAP is necessary and sufficient for ectopic mineralization, less clear are the factors inducing ectopic *ALPL* gene expression in non-bony tissue and cells. The objective of this study was to delineate the mechanism by which a lack of CD73-mediated adenosine signaling promotes calcification by upregulating expression of *ALPL* and activity of its protein product, TNAP.

MATERIALS & METHODS

The data that support the findings of this study are available from the corresponding author upon reasonable request. All patient samples were collected from individuals enrolled in studies that had been approved by the institutional review boards of the National Institutes of Health (control and ACDC cell lines), or procured from tissue donors after obtaining consent from next of kin according to protocols approved by the Nebraska Organ Recovery System (NORS).[5, 15] Tables 1 and 3 describe patient characteristics.

Cell Culture

Four human Control (CT) and five human ACDC dermal fibroblast cultures were obtained from patient punch biopsy and grown in Dulbecco's Modified Eagle's Medium (DMEM) supplemented with 20% fetal bovine serum (FBS) and 1X penicillin-streptomycin (P/S). Primary fibroblasts were used between passages 5 and 16. Growth media was changed every three days and cells were split 1:2 when confluent. Post-expansion, all cells were plated with either 250,000 cells per 9.5 cm^2, 125,000 cells per 4 cm^2, or 75,000 cells per 1.7 cm^2 with serum reduced to 10%. For cells undergoing osteogenic assay (also called in vitro disease model), no treatment media consisted of Gibco Minimum Essential Medium alpha + nucleosides supplemented with 10% FBS and 1X P/S while osteogenic treatment media consisted of no treatment media base with 10mM beta glycerol phosphate, 50μM ascorbic acid 2-phosphate, and 100nM dexamethasone made fresh. Growth media was removed before the assay, and media was changed every four days throughout the time course.

In experiments with exogenous AMP stimulation, cells were pretreated for 30 min with an adenosine deaminase inhibitor (EHNA 10μM), then treated with vehicle or 100μM exogenous AMP for 10 min. Forskolin and 3-isobutyl-1-methylxanthine (IBMX) were each used at a concentration of 10μM with EHNA for pretreatment and with AMP for treatment. Cells were counted by staining with 0.4% Trypan Blue stain. Live/dead analysis was performed using the ReadyProbes™ Cell Viability Imaging Kit, Blue/Green (Invitrogen) and the Life Technologies Countess II FL according to manufacturer's protocol.

All chemicals were dissolved in DMSO which was administered in equal volume as vehicle control. Rapamycin (200nM) was administered daily. D11 and L11 peptides were prepared according to manufacturer's protocols (Novus Biologicals) and used at a concentration of 10μM with treatment every two days. AS-1842856 was used at a concentration of 1uM. 8-Br-cAMP was used at a concentration of 0.5mM. CGS-21680 was used at a concentration of 10uM. BAY-60–6583 was used at a concentration of 10uM. In 5-day experiments, drugs were administered daily, and in 21-day assays, cells were treated every other day.

In autophagy flux experiments, confluent cells were serum-starved for 24–48hrs in DMEM supplemented with 0.5% FBS. Cells were then treated with normal growth media or HBSS (GIBCO) with 10nM bafilomycin (Sigma-Aldrich) or the same volume of DMSO as a vehicle control for four hours.

Transcriptional Analysis

RNA was extracted from cells using the RNeasy® Mini Kit (Qiagen) and complementary DNA (cDNA) was prepared using the High-Capacity cDNA Reverse Transcription Kit (Thermo Fischer) according to manufacturer's protocols. Gene expression was quantified by real-time PCR reaction of 4ng/uL cDNA, 1X SYBR Green (Thermo Fisher), 1μM each forward & reverse primer and amplified using with the following parameters: 50°C for 2 minutes and then 95°C for 10 minutes followed by 40 cycles of 95°C for 20 seconds, 58°C for 20 seconds, 72°C for 1 minute on a CFX Connect Real-Time PCR System (Bio-Rad).

Western Blot Analysis

Cells were lysed in 1% CHAPS hydrate, 150mM sodium chloride, 25mM HEPES buffer supplemented with 1x protease and phosphatase inhibitor (Sigma-Aldrich). Cells were scraped into microcentrifuge tubes, vortexed for 10 minutes, freeze/thawed for 5–8 cycles, then centrifuged at 12,000 × g for 10 minutes at 4°C. Protein lysate was combined with 1x Pierce LDS Sample Buffer, Non-Reducing (ThermoFisher Scientific) and 1x NuPAGE Sample Reducing Agent (Novex), brought to equal volume with CHAPS buffer, and denatured at 95°C for 15 minutes. Electrophoresis was performed on a 4–20% TGX stain-free polyacrylamide gel (Bio-Rad) in 1x Tris/Glycine/SDS Buffer (Bio-Rad). Proteins were transferred onto a 0.2um nitrocellulose membrane in 1x Trans-Blot Turbo Transfer Buffer (Bio-Rad) at 2.5A and 25V for 15 minutes using the Trans-Blot Turbo Transfer System (Bio-Rad). The membrane was blocked in Odyssey blocking buffer (PBS) (Li-COR) and primary antibodies were incubated in Odyssey blocking buffer with 0.1% Tween 20. Membranes were washed in PBS with 0.1% Tween 20 before incubation with secondary antibodies. Membranes were imaged on an Odyssey CLx (LI-COR) and analyzed with Image Studio (Version 5.2, LI-COR) software. If blots were stripped, they were done so using 1x Restore Fluorescent Western Blot Stripping Buffer (Thermo Fisher) according to manufacturer's protocols, washed with PBS, and placed directly into the next primary antibody solution.

Cyclic AMP Assay

Cells were serum starved and then pretreated with 100μM IBMX for 30 minutes at 37°C prior to treatment with 30uM AMP for 15 minutes. Cells were lysed in 0.1M HCl and 0.5% Triton-X 100, and the Direct cAMP ELISA kit (Enzo) was used according to manufacturer's instructions.

Alizarin Red Staining

Cells were washed with PBS and fixed with 4% paraformaldehyde (PFA) (Electron Microscopy Sciences) for 15 minutes at room temperature. Cells were then washed twice with deionized water and covered with 40mM Alizarin Red S (Sigma-Aldrich) at pH 4.1 – 4.3 for 20 minutes at room temperature. Unincorporated dye was removed, and cells were washed 2–3 times with deionized water before images were acquired. After imaging, Alizarin Red S was extracted with 10% (v/v) acetic acid (Fisher Scientific) for 30 minutes, scraped into a microcentrifuge tube, vortexed, and then incubated at 85°C for 10 minutes. After chilling on ice for 5 minutes, the mixture was centrifuged at 20,000 × g for 15 minutes at 4°C. 500 μL of supernatant was transferred to a new tube and 10% (v/v) ammonium hydroxide (Fisher Scientific) was then added to the supernatant. Absorbance was read in triplicate at 405 nm using a 96-well plate spectrophotometer.

Tissue Non-specific Alkaline Phosphatase Activity Staining

Cells were washed with 2x PBS and fixed with 4% PFA for 10 minutes at room temperature, then washed once with PBS and once with water. TNAP staining was produced using the SIGMAFAST™ BCIP®/NBT tablet according to manufacturer's instructions.

Immunofluorescence Imaging and Quantification

Cells were washed with PBS, then fixed with 4% PFA prepared in PBS 0.5% Triton-X 100 for 15 minutes. Cells were washed three times with PBS, 0.5% Triton-X 100 for 5 minutes each, incubated at room temperature for 1 hour in blocking buffer (PBS, 0.5% Triton-X 100, 5% FBS), then incubated overnight at 4°C in primary antibody. Cells were washed with PBS, 0.1% TWEEN 20 three times for 5 minutes, then incubated with secondary antibody for 1 hour. Cells were washed three times for 5 min each with PBS, 0.1% TWEEN 20, then once with PBS, and then stained for 30 minutes with AlexaFluor488 Phalloidin (Molecular Probes) for f-actin. Cells were washed a final time with PBS for five minutes, then mounted with Fluoroshield Mounting Medium with DAPI (Abcam). Slides were imaged within 24 hours of mounting.

To visualize p62 accumulation and localization, the Premo™ Autophagy Sensor RFP-p62 reagent (Life Technologies) was used according to manufacturer's instructions, counter stained with AlexaFluor488 Phalloidin, and mounted with Fluoroshield Mounting Medium with DAPI (Abcam). Cells were imaged within 24 hours of mounting. In ImageJ, each image was split into blue, red, and green channels, and the pixel intensity of the red and blue channels was measured. RFP-p62 intensity of an image was normalized to DAPI intensity for that same image.

MitoSOX™ red reagent (Molecular Probes) was diluted to 5μM in media and added to cells in a 4-well chamber slide which were incubated in the dark for 10 minutes at 37°C. Slides were prepared as above with the addition of AlexaFluor488 Phalloidin (Molecular Probes) and then mounted with Fluoroshield Mounting Medium with DAPI and imaged within 24 hours.

To quantify immunofluorescent stains, ImageJ was used to split each image into red, green, and blue channels, and the pixel intensity of the red and blue (DAPI) channels was measured. The measured intensity of a given stain was normalized to DAPI intensity of that same image.

PCR Mutagenesis, Transfection, and Luciferase Assays

The pEZX-LvPG04 backbone plasmid contains the 1353 base pairs upstream of the ATG start site of the human *ALPL* gene (NM_000478) and this promoter sequence drives expression of Gaussia luciferase (Genecopoeia). QuickChange II XL Site-Directed Mutagenesis Kit (Agilent) was used to substitute the putative FOXO1 recognition site TGTTG with TATTA using forward primer: 5'-TCTGTCTCTGTGTCTGTTAATATATCTGG CTTTCTCTGGGTC-3' and reverse primer: 5'-GACCCAGAGAAAGCCAGATATATTAACAG ACACAGAGACAGA-3' according to manufacturer's protocol. Mutant plasmids were selected and confirmed by Sanger sequencing (Genewiz) and transfected into cells using the Lipofectamine LTX Reagent with PLUS Reagent (Invitrogen) according to manufacturer's protocols. Luciferase was quantified using the Secrete-Pair Dual Luminescence Assay Kit (Genecopoeia) according to manufacturer's protocols and normalized to SEAP secretion.

Von Kossa Staining

Slides with adhered paraffin histological sections were warmed to 65°C for one hour and then deparaffinized through xylene and graded alcohol baths before being placed in distilled water. The slides were then stained using the Von Kossa Method of Calcium Kit (Polysciences, 24633–1) according to manufacturer's instructions.

Immunofluorescent Staining on Paraffin Sections

Slides were warmed for one hour at 65°C and deparaffinized by xylene and graded alcohol baths, rehydrated in ddH2O and heated for 20 minutes in antigen unmasking solution (Vector Labs). Slides were cooled to room temperature, then washed with PBS for five minutes. The tissues were incubated in blocking buffer (PBS, 3% fish skin gelatin, 10% horse serum) for one hour, then incubated in primary antibody overnight. Tissues were washed three times for five minutes each in wash buffer (PBS, 3% fish skin gelatin, 0.1% TWEEN 20), then for five minutes in PBS. Tissues were incubated with secondary antibody covered from light for one hour, then washed with wash buffer three times for five minutes each. Tissues were mounted with Fluoroshield Mounting Medium with DAPI (Abcam) and imaged within 24 hours.

Statistics

Statistical analysis was performed with GraphPad Prism 8 (GraphPad Software, Inc) and data shown are means ± SD. Statistical analysis used, exact n values, biological replicates, and p values are stated within each figure legend. A p value equal to or less than 0.05 was considered significant.

RESULTS

Excess AMP induces aberrant signaling in CD73-deficient cells.

Inactivating mutations in CD73 render the enzyme incapable of converting extracellular AMP into adenosine and inorganic phosphate, thus CD73-deficient cells are exposed to an excess of AMP resulting in a concomitant reduction in adenosine and downstream adenosine receptor signaling (Figure 1A). Adenosine receptors are G-protein coupled receptors which were initially classified by their ability to pair with the Gαi (A1, A3) and Gαs (A2a, A2b) G-protein subunits to inhibit or induce, respectively, adenylyl cyclase production of cAMP.[16] We found no differences in expression of adenosine receptor genes between control and ACDC cells (Figure 1B). A cAMP ELISA assay showed exogenous AMP induced increased production of cAMP in control, but not CD73-deficient fibroblasts, indicative of adenosine primarily signaling via the A2a or A2b adenosine receptors (Figure 1C). As a consequence of elevated cAMP levels, control cells showed activation of vasodilator-stimulated phosphoprotein (VASP) (Figure 1D). In contrast, phosphorylation of VASP was not observed in CD73-deficient ACDC cells treated with exogenous AMP, instead these cells exhibited increased levels of phosphorylated AKT at T308 and S473 (Figure 1D). To determine if elevation of cAMP could prevent phosphorylation of AKT and therefore rescue the absence of CD73 activity, ACDC cells were pre-treated with the adenylyl cyclase agonist forskolin and the phosphodiesterase inhibitor IBMX. Direct activation of adenylyl cyclase

induced phosphorylation of VASP and importantly, attenuated phosphorylation of AKT at T308 and S473 in ACDC cells (Figure 1E). These data suggest that lack of CD73/adenosine receptor-mediated production of cAMP contributes to aberrant AKT activation.

Inducing autophagy reduces calcification but autophagy flux is not altered in CD73-deficient cells.

We previously observed that CD73-deficient iPSCs and iPSC-derived mesenchymal stem cells exhibit an accelerated osteogenic differentiation that was inhibited in vitro and in vivo with rapamycin.[13] AKT is an upstream regulator of many signaling pathways, including mammalian target of rapamycin (mTOR). Activation of mTOR by AKT decreases autophagy, and decreased autophagy induces stem cells to differentiate into osteoblasts as well as promotes the calcification of smooth muscle cells.[17, 18] We observed that the mTOR inhibitor rapamycin reduced *ALPL* gene expression and TNAP activity and prevented calcification of CD73-deficient cells (Figure 2A–C). As rapamycin can affect many signaling pathways, autophagy was directly stimulated with a cell-penetrating peptide of Beclin-1 (D11) which mirrored rapamycin's anti-calcification effects (Figure 2D), illustrating that inducing autophagy alone is sufficient to prevent calcification.[19]

We next wanted to determine whether there were alterations in autophagy in CD73-deficient cells at baseline and under osteogenic conditions. Neither overnight treatment of exogenous AMP nor serum starvation altered the levels of the autophagosome cargo protein p62, or the ratio of LC3-II/I, the autophagosome biogenesis protein (Supplemental Figure IA, B), and autophagy flux experiments show no differences between control and CD73-deficient cells (Supplemental Figure IC). Further, no differences were observed in the localization or intensity of a p62-RFP conjugate protein transfected into cells treated under osteogenic conditions (Supplemental Figure ID), and long-term treatment under osteogenic stimulation with or without rapamycin did not result in differences in p62 or LC3-II/I ratios in ACDC cells (Supplemental Figure IE). Importantly, ACDC cells show increased LC3-II/I ratios upon treatment with D11 which illustrates their ability for autophagosome biogenesis. We found that exogenous AMP did not alter cell proliferation of control and ACDC cells under baseline or exogenous AMP stimulation for 21 days (Supplemental Figure IIA). Comparison of the percentage of live/dead cells showed exogenous AMP increased the number of live control cells compared to untreated control cells, and this increase was also seen in untreated ACDC cells at day 6, however these differences were not seen at the day 15 and 21 timepoints (Supplemental Figure IIA). Exogenous AMP also did not induce ER stress response and did not activate AMPK (Supplemental Figure IIB, C), and the levels of mitochondrial oxidative stress at baseline and after 21 days of exogenous AMP showed no differences (Supplemental Figure ID). From these data we conclude that proliferation, apoptosis, or mitochondrial oxidative stress are not significant contributors to the calcification seen in CD73-deficient cells. In summary, while treatment with rapamycin or the Beclin-1 peptide can prevent calcification, we do not observe alterations in autophagy processes in CD73-deficient cells.

Exogenous AMP promotes FOXO1 nuclear localization in CD73-deficient cells.

Increased TNAP activity is one of the main features observed in CD73-deficient fibroblasts when these cells are stimulated with osteogenic medium as well as in ACDC patient tissue.[13] As TNAP is a key enzyme in ectopic mineralization, we sought to determine which transcription factors may contribute to activation of *ALPL* gene expression in the absence of CD73 activity. Using the TRANSFAC® database we screened 1350bp upstream of the transcriptional start site of the human *ALPL* gene (NM_ 000478) and identified 227 sites with both a core score and matrix score of 1, indicative of a high likelihood of being a functional binding site (Table 2).[20] Of interest was a site for Forkhead Box O protein, FOXO1, located 445 base pairs upstream of the transcriptional start site (Figure 3A). Treatment with exogenous AMP promoted the localization of FOXO1 to the nucleus in ACDC, but not control cells. This localization was prevented when cells were pre-treated with the cAMP analogue 8-Br-cAMP or by activation of the A2a and A2b adenosine receptors, which activate adenylyl cyclase (Figure 3B). FOXO1 can be regulated by a variety of kinases, and proteasome-dependent degradation of FOXO1 is thought to be dependent on AKT phosphorylation.[21, 22] While exogenous AMP activates AKT in CD73-deficient cells we could not detect significant differences in the levels of FOXO1 phosphorylation between control and ACDC whole cell lysates after 30 minutes of stimulation using whole-cell lysate (Supplementary Figure III). Together, these data suggest that in the absence of CD73-generated adenosine signaling via the A2a and A2b receptor, exogenous AMP promotes the nuclear localization of FOXO1.

FOXO1 inhibition reduces ALPL expression, TNAP activity, and calcification.

CD73-deficient ACDC cells increase *ALPL* gene expression when cultured under osteogenic conditions, and treatment with the FOXO1 inhibitor AS-1842856 (1 μM) reduced *ALPL* transcription (Figure 4A). Similarly, AS-1842856 treatment decreased TNAP enzymatic activity in CD73-deficient ACDC cells cultured under osteogenic conditions, and further prevented cells from calcifying in the 21-day osteogenic assay, (Figure 4B, C) illustrating that FOXO1 function is required for calcification in the absence of CD73.

Plasmid DNA harboring the Gaussia luciferase gene under the control of the human *ALPL* gene promoter (hALPL) was used to assess the role of the putative FOXO1 binding site located 445 base pairs upstream from the transcriptional start site. Transfection of hALPL into control and ACDC cells shows promoter activity is increased at day 5 in CD73-deficient ACDC cells (Figure 4D). In ACDC cells transfected with hALPL, pretreatment with 200nM rapamycin reduced AMP-induced hALPL activity compared to the vehicle control, mirroring results in Figure 2 (Figure 4E). Site-directed PCR mutagenesis was performed to change the putative FOXO1 binding site from TGTTGAC to TATTAAC. This mutation reduced promoter activity 63% in response to AMP treatment (Figure 4F), indicating that this site is operative in the expression of human *ALPL.*

CD73 is decreased and FOXO1 is increased in calcified femoropopliteal arteries.

Patients with CD73 deficiency exhibit extensive calcification and vessel tortuosity in their lower extremity arteries. While CD73 deficiency is a rare disease with only a handful of individuals identified, one overarching goal of studying the mechanisms driving ACDC

pathogenesis is to uncover novel pathways that may be operative in more common forms of medial artery calcification.[5, 23–28] To that end, paraffin embedded femoropopliteal arteries from twenty age-matched donors exhibiting calcification and no calcification were obtained,[15] and Von Kossa stain used to confirm calcification state. Staining for CD73, FOXO1, and TNAP was performed on adjacent sections (Figure 5). We found calcified arteries exhibited dramatically lower CD73 staining than control arteries. We also found that the levels of FOXO1 staining are significantly higher in the calcified areas of Von Kossa-positive calcified vessels than the control vessels. Importantly, when comparing non-calcified regions to calcified regions in Von Kossa-positive vessels, we found that FOXO1 staining was substantially decreased in non-calcified areas. While the differences between TNAP staining in control versus calcified vessels did not reach statistical significance, similar to FOXO1 staining, TNAP staining was higher in the calcified regions of Von Kossa-positive vessels compared non-calcified regions from Von Kossa-positive vessels. These data suggest that a CD73/FOXO1/TNAP axis may be operative in more common forms of non-atherosclerotic medial layer vascular calcification.

DISCUSSION

The initial discovery that inactivating mutations in the gene encoding for CD73 protein result in extensive non-atherosclerotic lower extremity medial layer calcification identified a novel pathway involved in vascular calcification. Several CD73 knockout mouse models are available and while these mice exhibit calcification in the juxta-articular spaces in their joints, similar to that seen in ACDC patients, there is no evidence of calcification in any of the vascular beds.[10,29–31] This underscores that vascular mineralization potential is very different in mice compared to humans, and justifies our use of primary human cells in an in vitro disease model to study the mechanism driving ACDC pathogenesis.[11] The cell source for this in vitro disease model is dermal fibroblasts, which is a limiting factor of this model. However, the use of fibroblasts in disease modeling has been well established,[32] and our published studies illustrate that this system is sufficient to recapitulate this calcification phenotype and therefore suitable to define the underlying mechanisms promoting the ectopic calcification phenotype seen in ACDC patients.

Two sites on AKT are considered to be rate-limiting for the propagation of downstream signaling; phosphorylation of AKT at T308 is mediated via PDK1, and S473 via mTORC2.[33] We have now shown that in the absence of CD73 activity, exogenous AMP induces phosphorylation of AKT at these sites, and this phosphorylation is mitigated when adenylyl cyclase is directly activated to produce cAMP (Figure 1). Our findings tie in nicely with previous biochemical studies which illustrated that cAMP inhibits AKT phosphorylation by blocking the localization of PDK1 to the cell membrane and inhibiting the lipid kinase activity of PI3K, and blocks insulin and amino acid starvation-induced mTORC1 activation.[34, 35] Additionally, a lack of cAMP production due to inactivating mutations in *GNAS*, the gene encoding for adenylyl cyclase, was found to contribute in the pathogenesis of another ectopic calcification disorder, progressive osseous heteroplasia. This coupled with our results suggests that reduced intracellular cAMP production may be shared in various forms dystrophic vascular calcification.[36] What remains to be determined is the mechanism through which exogenous AMP induces AKT phosphorylation. One report

suggests that AMP is able to signal through binding the A1 adenosine receptor. Experiments were conducted with physiological concentrations of exogenous AMP, however in this reporter system cells were transfected with plasmid DNA to overexpress the A1 adenosine receptor as well as the Gαi G-protein subunit.[37] The A1 adenosine receptor density on the cell surface as well as the internal Gαi were under constitutively active promoters and thus not present at physiological levels; thus evidence of a true AMP receptor in human cells or tissues is lacking.

To date, hundreds of AKT substrates have been identified and we became interested in the role of CD73 in regulating autophagy, as AKT activation can promote mTORC1-mediated inhibition of autophagy. While upregulated under stressed conditions such as nutrient deprivation, autophagy is active even at baseline and is necessary to ensure proper homeostasis. One study modeling chronic kidney disease-induced vascular calcification identified a link between the activation of autophagy and a means to prevent calcification.[18] We hypothesized that increased AMP-induced AKT activation may lead to reduced levels of autophagy which would promote calcification. Although AKT was phosphorylated in CD73-deficient cells we found no defect in autophagy flux.

Moving away from defects in autophagy, we conducted an in-silico screen of the human *ALPL* promoter and focused on a putative FOXO1 transcription factor binding site located 445 base pairs upstream of the *ALPL* transcriptional start site. Forkhead box transcription factors are an evolutionarily conserved family that in mammals regulate a wide array of cellular processes, including proliferation, apoptosis, metabolism and oxidative stress resistance.[21] Their necessity in development was illustrated first in *Drosophila*, and *FoxO1* knockout mice die around embryonic day 11 primarily due to defects in vascular development in the embryo and yolk sac.[38, 39] While necessary in development, in disease states FOXO transcription factors can contribute to disease pathology. For example, increased FOXO1 signaling in liver and pancreatic cells induces diabetes via impairing insulin signaling.[40] There have been various and opposing reports of these transcription factors in osteogenesis and ectopic calcification. In vitro and in vivo genetic knockdown shows that FOXO1 helps drive the differentiation of mesenchymal stem cells into osteoblasts, and bone-specific knockout murine models provide evidence that FOXO1 is necessary for osteoblast function and bone homeostasis.[41, 42] In opposition to these studies in bone, in mice harboring a smooth muscle cell-specific deletion of *Pten gene* (phosphatase and tensin homolog), loss of PTEN promoted calcification by stabilizing RUNX2 protein levels which are normally targeted for ubiquitination and proteasome mediated degradation via FOXO1 and FOXO3.[43] PTEN is a phosphatase that acts on AKT to inhibit AKT signaling, thus these mice exhibit constitutively active AKT in their smooth muscle cells. In our human system we observe elevated AKT activation in response to exogenous AMP.

While RUNX2 is a regulator of genes necessary for the osteogenic transition of stem and vascular smooth muscle cells,[44–47] there is evidence for RUNX2-independent upregulation of *ALPL* in response to some osteogenic stimuli. Specifically, TNF-α and IL-1β decreased *RUNX2* expression in human mesenchymal stem cells but increased expression of *ALPL,* and this increase of *ALPL* and subsequent TNAP activity is sufficient to induce calcification.[48] The necessity of functional TNAP is clear in both humans and mice, where

genetic mutation or deletion of the *ALPL* gene causes hypophosphatasia, also known as rickets, and one study found that FOXO1 binds and activates murine *Alpl* promoter, which supports our finding on the role of FOXO1 in activating *ALPL* promoter activity in human cells.[49–51] Our data show that in the absence of CD73 activity AMP induces FOXO1 nuclear localization which stimulates *ALPL* promoter activation; nuclear localization of FOXO1 is prevented when cAMP levels are increased.

Lastly, our data suggest that mechanisms driving ACDC pathogenesis may contribute to calcification in non-ACDC peripheral arteries. Calcification in the lower extremity arteries is relatively common and can present alongside or independent of atherosclerosis. Differences in calcification properties and patterns have been observed in the vascular beds. Carotid artery calcification is most commonly found in the necrotic core of atherosclerotic plaques, while lower-extremity calcification is often plaque-independent and localizes in the medial layer along the elastic fibers[15, 52]. Carotid, femoral, and femoropopliteal arteries exhibit microcalcification, sheet calcification, and nodular calcification, however the lower extremity vessels exhibited true bone formation (osteoid metaplasia), indicative of a cell phenotypic switching from a vascular to an osteogenic-type cell.[53] Supporting this, lower-extremity arteries exhibited elevated expression of bone development genes, and relevant to our findings, *ENPP1*, the enzyme directly upstream of CD73 that converts extracellular ATP to AMP, was found to be drastically downregulated in lower limb arteries, suggesting that its absence may contribute to decreases in the available adenosine.

The femoropopliteal artery of mobile individuals experiences mechanical stretches and stresses during limb flexion which may induce cells to release ATP.[54] ATP in the extracellular space is rapidly converted to adenosine when CD73 is present, and this adenosine helps protect cells from this stress, hence the notion that adenosine is a “retaliatory metabolite”.[55] Calcified femoropopliteal arteries exhibit medial remodeling and are stiffer in both longitudinal and circumferential directions.[15] A recent study classified 431 femoropopliteal artery samples into seven groups that histologically exhibit varying degrees of calcification and found that stiffness precedes evidence of extensive calcification[15] Mechanical stretch can induce the expression of CD73 on lung epithelial cells and the adenosine generated is protective against acute lung injury.[56] We found robust staining for CD73 in control femoropopliteal arteries, however CD73 was nearly absent in calcified arteries. We found that calcified femoropopliteal arteries exhibit lower levels of CD73. Future studies will explore whether stiffness decreases CD73 expression and whether aberrant CD73/adenosine receptor signaling precedes calcification in non-ACDC contexts.

From these studies and our observations, we postulate that CD73-mediated adenosine signaling may protect the femoropopliteal artery during mechanical stretch; thus, a reduction of CD73 would prevent this protection. What is clear from our data is that the study of this rare monogenetic disease is able to inform us about potential novel mechanisms operative in more common forms of peripheral medial layer vascular calcification.

Supplementary Material

Refer to Web version on PubMed Central for supplementary material.

ACKNOWLEDGEMENTS

We would like to thank Jason Dobbins for insightful discussion and critical reading of this manuscript. We would also like to acknowledge Live On Nebraska for their help and support, and thank tissue donors and their families for making this study possible. Some figures created with Biorender.com.

SOURCES OF FUNDING

CS is supported by the National Heart, Lung, and Blood Institute K22 HL117917, the Pittsburgh Heart, Lung, and Blood Vascular Medicine Institute, and the University of Pittsburgh School of Medicine Division of Cardiology. AK and JM were funded in part by the National Heart, Lung, And Blood Institute of the National Institutes of Health under Award Numbers HL125736 and HL147128.

ABBREVIATIONS

ACDC	Arterial Calcification due to Deficiency of CD73
AMPK	AMP-activated protein kinase
CT	control
D11	Tat-Beclin 1 peptide
FBS	fetal bovine serum
FOXO1	forkhead box O1 protein
iPSC	induced pluripotent stem cell
L11	Tat-Beclin 1 L11
LC3	microtubule-associated protein 1A/1B-light chain 3
mTOR	mammalian target of rapamycin
P/S	penicillin-streptomycin
TNAP	tissue non-specific alkaline phosphatase
VASP	vasodilator-stimulated phosphoprotein

REFERENCES

1. Detrano R, Guerci AD, Carr JJ, Bild DE, Burke G, Folsom AR, Liu K, Shea S, Szklo M, Bluemke DA, O'Leary DH, Tracy R, Watson K, Wong ND, Kronmal RA. Coronary calcium as a predictor of coronary events in four racial or ethnic groups. N Engl J Med. 2008;358:1336–1345 [PubMed: 18367736]
2. Lanzer P, Boehm M, Sorribas V, Thiriet M, Janzen J, Zeller T, St Hilaire C, Shanahan C. Medial vascular calcification revisited: Review and perspectives. Eur Heart J. 2014;35:1515–1525 [PubMed: 24740885]
3. St Hilaire C, Liberman M, Miller JD, Early Career C. Bidirectional translation in cardiovascular calcification. Arterioscler Thromb Vasc Biol. 2016;36:e19–24 [PubMed: 26912744]
4. Rutsch F, Ruf N, Vaingankar S, Toliat MR, Suk A, Hohne W, Schauer G, Lehmann M, Roscioli T, Schnabel D, Epplen JT, Knisely A, Superti-Furga A, McGill J, Filippone M, Sinaiko AR, Vallance H, Hinrichs B, Smith W, Ferre M, Terkeltaub R, Nurnberg P. Mutations in enpp1 are associated with 'idiopathic' infantile arterial calcification. Nat Genet. 2003;34:379–381 [PubMed: 12881724]

5. St Hilaire C, Ziegler SG, Markello TC, Brusco A, Groden C, Gill F, Carlson-Donohoe H, Lederman RJ, Chen MY, Yang D, Siegenthaler MP, Arduino C, Mancini C, Freudenthal B, Stanescu HC, Zdebik AA, Chaganti RK, Nussbaum RL, Kleta R, Gahl WA, Boehm M. Nt5e mutations and arterial calcifications. N Engl J Med. 2011;364:432–442 [PubMed: 21288095]
6. Lohman AW, Billaud M, Isakson BE. Mechanisms of atp release and signalling in the blood vessel wall. Cardiovasc Res. 2012;95:269–280 [PubMed: 22678409]
7. Otto CM, Prendergast B. Aortic-valve stenosis--from patients at risk to severe valve obstruction. N Engl J Med. 2014;371:744–756 [PubMed: 25140960]
8. Sauer H, Hescheler J, Wartenberg M. Mechanical strain-induced ca(2+) waves are propagated via atp release and purinergic receptor activation. Am J Physiol Cell Physiol. 2000;279:C295–307 [PubMed: 10912995]
9. Murata N, Ito S, Furuya K, Takahara N, Naruse K, Aso H, Kondo M, Sokabe M, Hasegawa Y. Ca2+ influx and atp release mediated by mechanical stretch in human lung fibroblasts. Biochem Biophys Res Commun. 2014;453:101–105 [PubMed: 25256743]
10. Li Q, Price TP, Sundberg JP, Uitto J. Juxta-articular joint-capsule mineralization in cd73 deficient mice: Similarities to patients with nt5e mutations. Cell Cycle. 2014;13:2609–2615 [PubMed: 25486201]
11. Joolharzadeh P, St Hilaire C. Cd73 (cluster of differentiation 73) and the differences between mice and humans. Arterioscler Thromb Vasc Biol. 2019;39:339–348 [PubMed: 30676071]
12. Markello TC, Pak LK, St Hilaire C, Dorward H, Ziegler SG, Chen MY, Chaganti K, Nussbaum RL, Boehm M, Gahl WA. Vascular pathology of medial arterial calcifications in nt5e deficiency: Implications for the role of adenosine in pseudoxanthoma elasticum. Mol Genet Metab. 2011;103:44–50 [PubMed: 21371928]
13. Jin H, St Hilaire C, Huang Y, Yang D, Dmitrieva NI, Negro A, Schwartzbeck R, Liu Y, Yu Z, Walts A, Davaine JM, Lee DY, Donahue D, Hsu KS, Chen J, Cheng T, Gahl W, Chen G, Boehm M. Increased activity of tnap compensates for reduced adenosine production and promotes ectopic calcification in the genetic disease acdc. Sci Signal. 2016;9:ra121 [PubMed: 27965423]
14. Hessle L, Johnson KA, Anderson HC, Narisawa S, Sali A, Goding JW, Terkeltaub R, Millan JL. Tissue-nonspecific alkaline phosphatase and plasma cell membrane glycoprotein-1 are central antagonistic regulators of bone mineralization. Proc Natl Acad Sci U S A. 2002;99:9445–9449 [PubMed: 12082181]
15. Kamenskiy A, Poulson W, Sim S, Reilly A, Luo J, MacTaggart J. Prevalence of calcification in human femoropopliteal arteries and its association with demographics, risk factors, and arterial stiffness. Arterioscler Thromb Vasc Biol. 2018
16. St. Hilaire C, Yang D, Schreiber BM, Ravid K. B-myb regulates the a(2b) adenosine receptor in vascular smooth muscle cells. Journal of Cellular Biochemistry. 2008;103:1962–1974 [PubMed: 17979185]
17. Oliver L, Hue E, Priault M, Vallette FM. Basal autophagy decreased during the differentiation of human adult mesenchymal stem cells. Stem Cells Dev. 2012;21:2779–2788 [PubMed: 22519885]
18. Dai XY, Zhao MM, Cai Y, Guan QC, Zhao Y, Guan Y, Kong W, Zhu WG, Xu MJ, Wang X. Phosphate-induced autophagy counteracts vascular calcification by reducing matrix vesicle release. Kidney Int. 2013;83:1042–1051 [PubMed: 23364520]
19. Shoji-Kawata S, Sumpter R, Leveno M, Campbell GR, Zou Z, Kinch L, Wilkins AD, Sun Q, Pallauf K, MacDuff D, Huerta C, Virgin HW, Helms JB, Eerland R, Tooze SA, Xavier R, Lenschow DJ, Yamamoto A, King D, Lichtarge O, Grishin NV, Spector SA, Kaloyanova DV, Levine B. Identification of a candidate therapeutic autophagy-inducing peptide. Nature. 2013;494:201–206 [PubMed: 23364696]
20. Matys V, Kel-Margoulis OV, Fricke E, Liebich I, Land S, Barre-Dirrie A, Reuter I, Chekmenev D, Krull M, Hornischer K, Voss N, Stegmaier P, Lewicki-Potapov B, Saxel H, Kel AE, Wingender E. Transfac and its module transcompel: Transcriptional gene regulation in eukaryotes. Nucleic Acids Res. 2006;34:D108–110 [PubMed: 16381825]
21. van der Horst A, Burgering BM. Stressing the role of foxo proteins in lifespan and disease. Nat Rev Mol Cell Biol. 2007;8:440–450 [PubMed: 17522590]

22. Huang H, Tindall DJ. Dynamic foxo transcription factors. Journal of cell science. 2007;120:2479–2487 [PubMed: 17646672]
23. de Nijs T, Albuisson J, Ockeloen CW, Legrand A, Jeunemaitre X, Schultze Kool LJ, Riksen NP. Isolated arterial calcifications of the lower extremities: A clue for nt5e mutation. Int J Cardiol. 2016;212:248–250 [PubMed: 27045881]
24. Ichikawa N, Taniguchi A, Kaneko H, Kawamoto M, Sekita C, Nakajima A, Yamanaka H. Arterial calcification due to deficiency of cd73 (acdc) as one of rheumatic diseases associated with periarticular calcification. J Clin Rheumatol. 2015;21:216–220 [PubMed: 26010187]
25. Kochan Z, Karbowska J, Gogga P, Kutryb-Zajac B, Slominska EM, Smolenski RT. Polymorphism in exon 6 of the human nt5e gene is associated with aortic valve calcification. Nucleosides Nucleotides Nucleic Acids. 2016;35:726–731 [PubMed: 27906615]
26. Rothe H, Brandenburg V, Haun M, Kollerits B, Kronenberg F, Ketteler M, Wanner C. Ecto-5' -nucleotidase cd73 (nt5e), vitamin d receptor and fgf23 gene polymorphisms may play a role in the development of calcific uremic arteriolopathy in dialysis patients - data from the german calciphylaxis registry. PLoS One. 2017;12:e0172407 [PubMed: 28212442]
27. Yoshioka K, Kuroda S, Takahashi K, Sasano T, Furukawa T, Matsumura A. Calcification of joints and arteries with novel nt5e mutations with involvement of upper extremity arteries. Vasc Med. 2017;22:541–543 [PubMed: 28825389]
28. Zhang Z, He JW, Fu WZ, Zhang CQ, Zhang ZL. Calcification of joints and arteries: Second report with novel nt5e mutations and expansion of the phenotype. J Hum Genet. 2015;60:561–564 [PubMed: 26178434]
29. Koszalka P, Ozuyaman B, Huo Y, Zernecke A, Flogel U, Braun N, Buchheiser A, Decking UK, Smith ML, Sevigny J, Gear A, Weber AA, Molojavyi A, Ding Z, Weber C, Ley K, Zimmermann H, Godecke A, Schrader J. Targeted disruption of cd73/ecto-5'-nucleotidase alters thromboregulation and augments vascular inflammatory response. Circ Res. 2004;95:814–821 [PubMed: 15358667]
30. Thompson LF, Eltzschig HK, Ibla JC, Van De Wiele CJ, Resta R, Morote-Garcia JC, Colgan SP. Crucial role for ecto-5'-nucleotidase (cd73) in vascular leakage during hypoxia. J Exp Med. 2004;200:1395–1405 [PubMed: 15583013]
31. Castrop H, Huang Y, Hashimoto S, Mizel D, Hansen P, Theilig F, Bachmann S, Deng C, Briggs J, Schnermann J. Impairment of tubuloglomerular feedback regulation of gfr in ecto-5'-nucleotidase/cd73-deficient mice. J Clin Invest. 2004;114:634–642 [PubMed: 15343381]
32. Brown MS, Goldstein JL. Analysis of a mutant strain of human fibroblasts with a defect in the internalization of receptor-bound low density lipoprotein. Cell. 1976;9:663–674 [PubMed: 189940]
33. Manning BD, Toker A. Akt/pkb signaling: Navigating the network. Cell. 2017;169:381–405 [PubMed: 28431241]
34. Kim S, Jee K, Kim D, Koh H, Chung J. Cyclic amp inhibits akt activity by blocking the membrane localization of pdk1. J Biol Chem. 2001;276:12864–12870 [PubMed: 11278269]
35. Xie J, Ponuwei GA, Moore CE, Willars GB, Tee AR, Herbert TP. Camp inhibits mammalian target of rapamycin complex-1 and −2 (mtorc1 and 2) by promoting complex dissociation and inhibiting mtor kinase activity. Cell Signal. 2011;23:1927–1935 [PubMed: 21763421]
36. Adegbite NS, Xu M, Kaplan FS, Shore EM, Pignolo RJ. Diagnostic and mutational spectrum of progressive osseous heteroplasia (poh) and other forms of gnas-based heterotopic ossification. Am J Med Genet A. 2008;146A:1788–1796 [PubMed: 18553568]
37. Rittiner JE, Korboukh I, Hull-Ryde EA, Jin J, Janzen WP, Frye SV, Zylka MJ. Amp is an adenosine a1 receptor agonist. J Biol Chem. 2012;287:5301–5309 [PubMed: 22215671]
38. Furuyama T, Kitayama K, Shimoda Y, Ogawa M, Sone K, Yoshida-Araki K, Hisatsune H, Nishikawa S, Nakayama K, Nakayama K, Ikeda K, Motoyama N, Mori N. Abnormal angiogenesis in foxo1 (fkhr)-deficient mice. J Biol Chem. 2004;279:34741–34749 [PubMed: 15184386]
39. Weigel D, Jurgens G, Kuttner F, Seifert E, Jackle H. The homeotic gene fork head encodes a nuclear protein and is expressed in the terminal regions of the drosophila embryo. Cell. 1989;57:645–658 [PubMed: 2566386]

40. Nakae J, Biggs WH 3rd, Kitamura T, Cavenee WK, Wright CV, Arden KC, Accili D. Regulation of insulin action and pancreatic beta-cell function by mutated alleles of the gene encoding forkhead transcription factor foxo1. Nat Genet. 2002;32:245–253 [PubMed: 12219087]
41. Teixeira CC, Liu Y, Thant LM, Pang J, Palmer G, Alikhani M. Foxo1, a novel regulator of osteoblast differentiation and skeletogenesis. J Biol Chem. 2010;285:31055–31065 [PubMed: 20650891]
42. Rached MT, Kode A, Xu L, Yoshikawa Y, Paik JH, Depinho RA, Kousteni S. Foxo1 is a positive regulator of bone formation by favoring protein synthesis and resistance to oxidative stress in osteoblasts. Cell Metab. 2010;11:147–160 [PubMed: 20142102]
43. Deng L, Huang L, Sun Y, Heath JM, Wu H, Chen Y. Inhibition of foxo1/3 promotes vascular calcification. Arterioscler Thromb Vasc Biol. 2015;35:175–183 [PubMed: 25378413]
44. Lee KS, Kim HJ, Li QL, Chi XZ, Ueta C, Komori T, Wozney JM, Kim EG, Choi JY, Ryoo HM, Bae SC. Runx2 is a common target of transforming growth factor beta1 and bone morphogenetic protein 2, and cooperation between runx2 and smad5 induces osteoblast-specific gene expression in the pluripotent mesenchymal precursor cell line c2c12. Mol Cell Biol. 2000;20:8783–8792 [PubMed: 11073979]
45. Byon CH, Sun Y, Chen J, Yuan K, Mao X, Heath JM, Anderson PG, Tintut Y, Demer LL, Wang D, Chen Y. Runx2-upregulated receptor activator of nuclear factor kappab ligand in calcifying smooth muscle cells promotes migration and osteoclastic differentiation of macrophages. Arterioscler Thromb Vasc Biol. 2011;31:1387–1396 [PubMed: 21454810]
46. Zhang J, Zheng B, Zhou PP, Zhang RN, He M, Yang Z, Wen JK. Vascular calcification is coupled with phenotypic conversion of vascular smooth muscle cells through klf5-mediated transactivation of the runx2 promoter. Biosci Rep. 2014;34:e00148 [PubMed: 25205373]
47. Lin ME, Chen T, Leaf EM, Speer MY, Giachelli CM. Runx2 expression in smooth muscle cells is required for arterial medial calcification in mice. Am J Pathol. 2015;185:1958–1969 [PubMed: 25987250]
48. Ding J, Ghali O, Lencel P, Broux O, Chauveau C, Devedjian JC, Hardouin P, Magne D. Tnf-alpha and il-1beta inhibit runx2 and collagen expression but increase alkaline phosphatase activity and mineralization in human mesenchymal stem cells. Life Sci. 2009;84:499–504 [PubMed: 19302812]
49. Fedde KN, Blair L, Silverstein J, Coburn SP, Ryan LM, Weinstein RS, Waymire K, Narisawa S, Millan JL, MacGregor GR, Whyte MP. Alkaline phosphatase knockout mice recapitulate the metabolic and skeletal defects of infantile hypophosphatasia. J Bone Miner Res. 1999;14:2015–2026 [PubMed: 10620060]
50. Weiss MJ, Cole DE, Ray K, Whyte MP, Lafferty MA, Mulivor RA, Harris H. A missense mutation in the human liver/bone/kidney alkaline phosphatase gene causing a lethal form of hypophosphatasia. Proc Natl Acad Sci U S A. 1988;85:7666–7669 [PubMed: 3174660]
51. Hatta M, Daitoku H, Matsuzaki H, Deyama Y, Yoshimura Y, Suzuki K, Matsumoto A, Fukamizu A. Regulation of alkaline phosphatase promoter activity by forkhead transcription factor fkhr. Int J Mol Med. 2002;9:147–152 [PubMed: 11786925]
52. Yahagi K, Kolodgie FD, Otsuka F, Finn AV, Davis HR, Joner M, Virmani R. Pathophysiology of native coronary, vein graft, and in-stent atherosclerosis. Nat Rev Cardiol. 2016;13:79–98 [PubMed: 26503410]
53. Steenman M, Espitia O, Maurel B, Guyomarch B, Heymann M-F, Pistorius M-A, Ory B, Heymann D, Houlgatte R, Gouëffic Y, Quillard T. Identification of genomic differences among peripheral arterial beds in atherosclerotic and healthy arteries. Scientific Reports. 2018;8:3940 [PubMed: 29500419]
54. Mikolajewicz N, Mohammed A, Morris M, Komarova SV. Mechanically stimulated atp release from mammalian cells: Systematic review and meta-analysis. Journal of cell science. 2018;131
55. Newby AC. Adenosine and the concept of ‘retaliatory metabolites’. Trends in Biochemical Sciences. 1984;9:42–44
56. Eckle T, Fullbier L, Wehrmann M, Khoury J, Mittelbronn M, Ibla J, Rosenberger P, Eltzschig HK. Identification of ectonucleotidases cd39 and cd73 in innate protection during acute lung injury. J Immunol. 2007;178:8127–8137 [PubMed: 17548651]

HIGHLIGHTS

- In the absence of CD73 activity and downstream adenosine signaling, exogenous AMP induces phosphorylation of AKT, nuclear localization of FOXO1, and promotes expression and activity of *ALPL*/TNAP.
- CD73 expression is decreased in a calcified femoropopliteal arteries compared to control samples
- Within the same vessel, calcified areas exhibit increased FOXO1 and TNAP staining than in non-calcified areas.

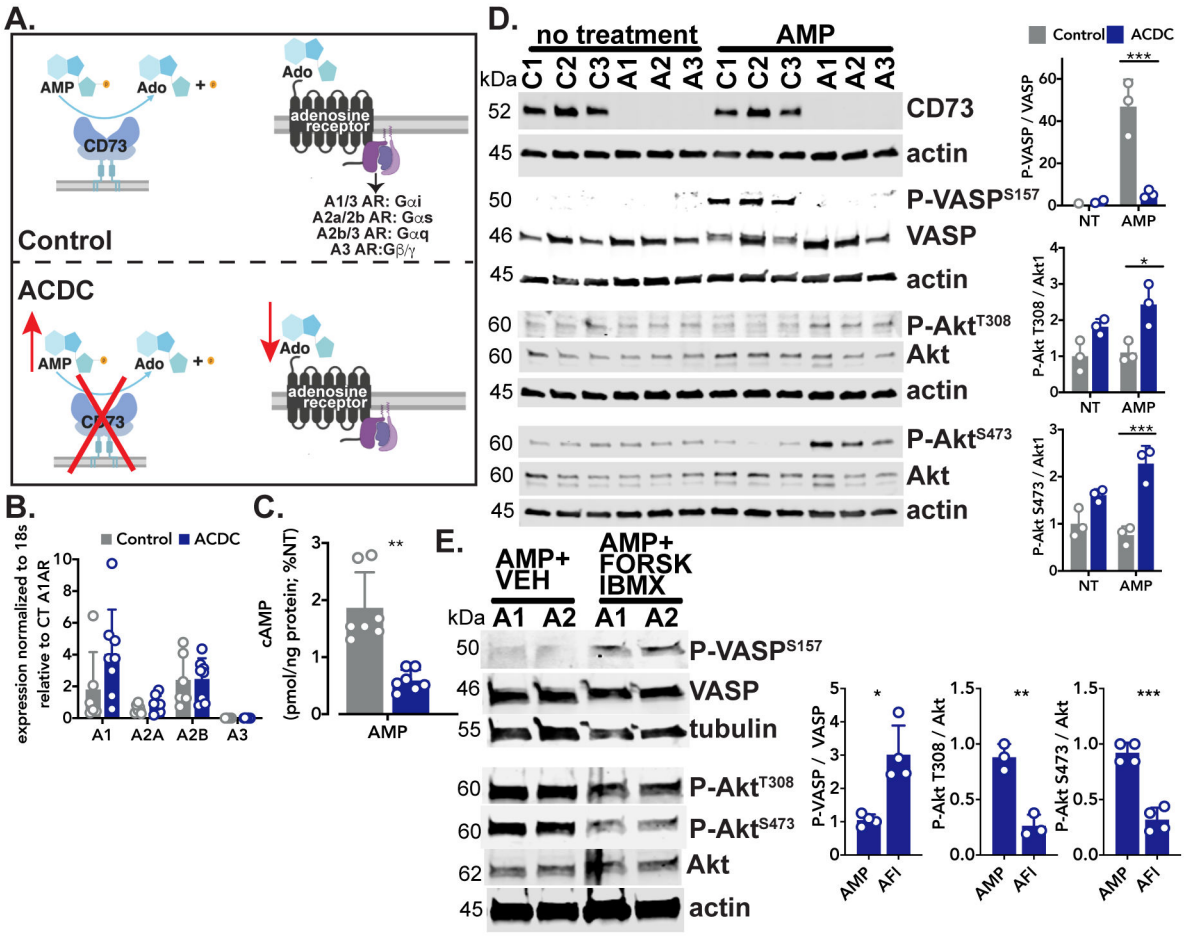

FIGURE 1: AMP induces aberrant signaling in ACDC cells.

A. Schematic of CD73 and downstream adenosine receptor signaling. **B.** Baseline measurement of adenosine receptor gene expression. Results representative of n=6–8 per group using 4 control and 3 ACDC patient cell lines. Statistical analysis performed using unpaired t test with Welch's correction. **C.** Quantification of cAMP levels in control and ACDC cells in response to exogenous AMP. Cells were pretreated with 0.5 mM IBMX for 30 minutes then treated with 30μM AMP for 15 minutes. Results representative of n=7 per group using 3 control and 4 ACDC patient cell lines. **p=0.0013 using unpaired t test with Welch's correction. **D.** Control and ACDC fibroblasts were given exogenous 100μM AMP for 10 minutes and total cell lysates were analyzed by western blotting for VASP and AKT phosphorylation. Results representative of n=3 per group using 3 Control patient and 3 ACDC patient cell lines. For P-VASP ***p=0.0003, P- AKT T308 *p=0.0155, P- AKT S473 ***p=0.0005. Two-way ANOVA with Tukey's multiple comparisons test was used for statistical analysis. **E.** ACDC fibroblasts were treated with 100μM exogenous AMP or pretreated with 10μM forskolin and 10μM IBMX for 30 minutes before treatment with 100μM exogenous AMP, 10μM forskolin, and 10μM IBMX (AFI) for 10 minutes. Total cell lysates were analyzed by western blotting for VASP and AKT phosphorylation. Results representative of n=3–4 per group using 2 ACDC patient cell lines. For P-VASP *p=0.0183,

P-AKT T308 **p=0.0025, P-AKT S473 ***p=0.0002. One-way ANOVA with Tukey's multiple comparisons test was used for statistical analysis.

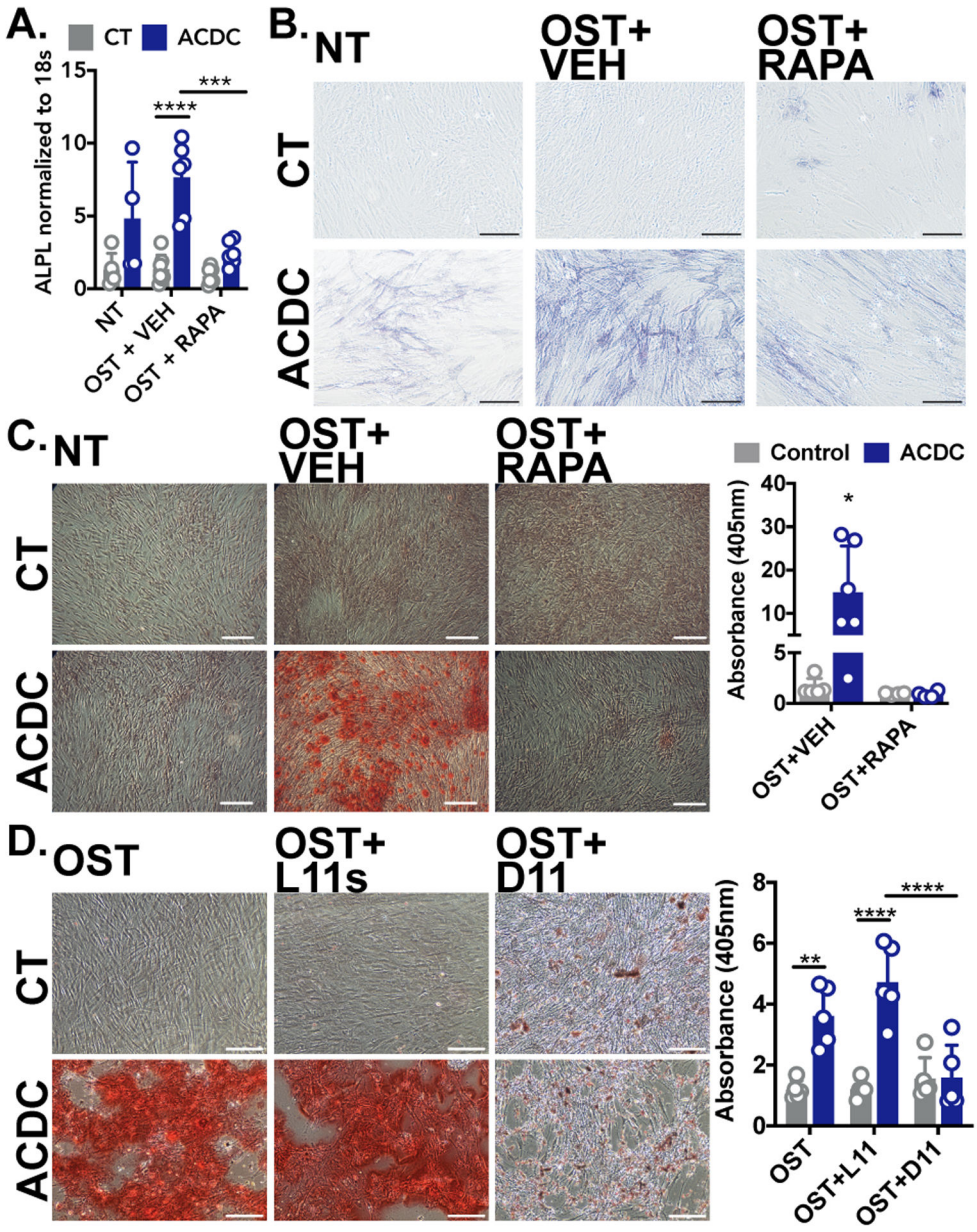

FIGURE 2: Inducing autophagy reduces calcification in CD73-deficient cells.

A. *ALPL* gene expression. Results representative of n=4–7 per group using 3 control and 3 ACDC patient cell lines. ***p=0.003 ****p=<0.0001 **B.** Staining for TNAP activity in control and ACDC fibroblasts cultured in osteogenic media and supplemented with 200nM rapamycin for 5 days. Results representative of n=4–7 per group using 3 control and 3 ACDC patient cell lines. **C.** Alizarin Red S stain was used to image and quantify calcification content in control and ACDC fibroblasts cultured under osteogenic conditions for 21 days and supplemented with 200nM rapamycin. Results representative of n=6 per group using 2 control and 2 ACDC patient cell lines. *p=0.037. **D.** Alizarin Red S staining of control and ACDC cells treated with autophagy-inducing peptide Tat-Beclin 1 D11. Results representative of n=5 per group using 4 control and 3 ACDC patient cell lines.

**p=0.0043 ****p<0.0001. Scale bar represents 200um. Two-way ANOVA with Tukey's multiple comparisons test was used for all statistical analyses in this figure.

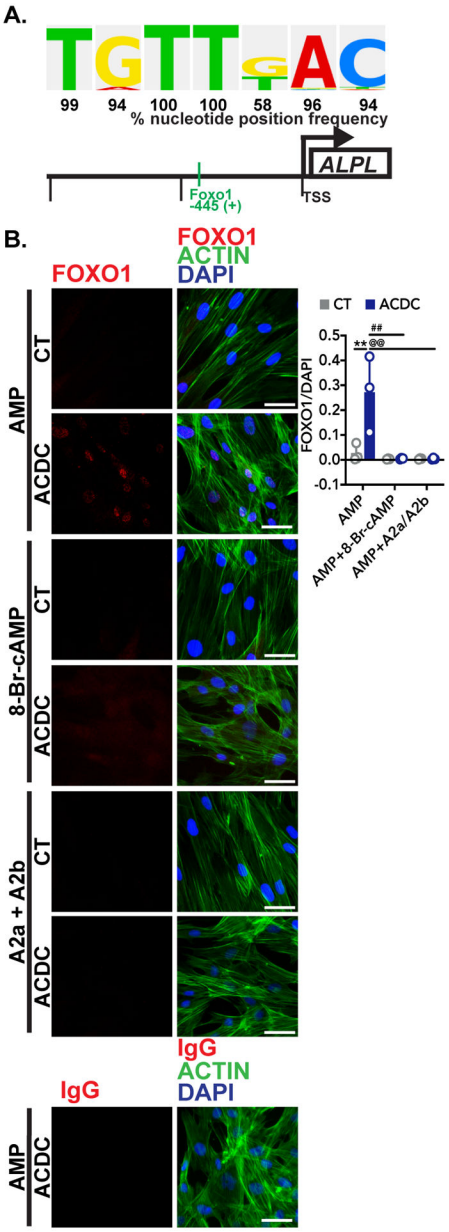

FIGURE 3: AMP induces FOXO1 nuclear localization.

A. The putative FOXO1 binding site in the human *ALPL* promoter shown with the percentage that the sequence located 445 upstream of the transcriptional start site (TSS) on the human *ALPL* promoter is found in experimentally proven FOXO1 binding sites according to the TRANSFAC® database. **B.** Immunofluorescent staining was used to detect FOXO1 localization in response to exogenous AMP. Control and ACDC fibroblasts were pretreated with vehicle, 0.5mM 8-Br-cAMP, or 10μM each of CGS-21680 and BAY 60–6583 (A2a and A2b agonists, respectively) for 30 minutes, then 100μM AMP was added to each group for 2 hours. Cells were stained with anti-FOXO1 antibody and an IgG control, and pixel intensity was quantified and normalized to DAPI. **p=0.0054, ##p=0.0027, @@p=0.0027 using two-way ANOVA with Tukey's multiple comparisons test for statistical

analysis. Results representative of 5 replicates of 3 control patient cell lines and 3 ACDC patient cell lines per group. Scale bar represents 50 μm.

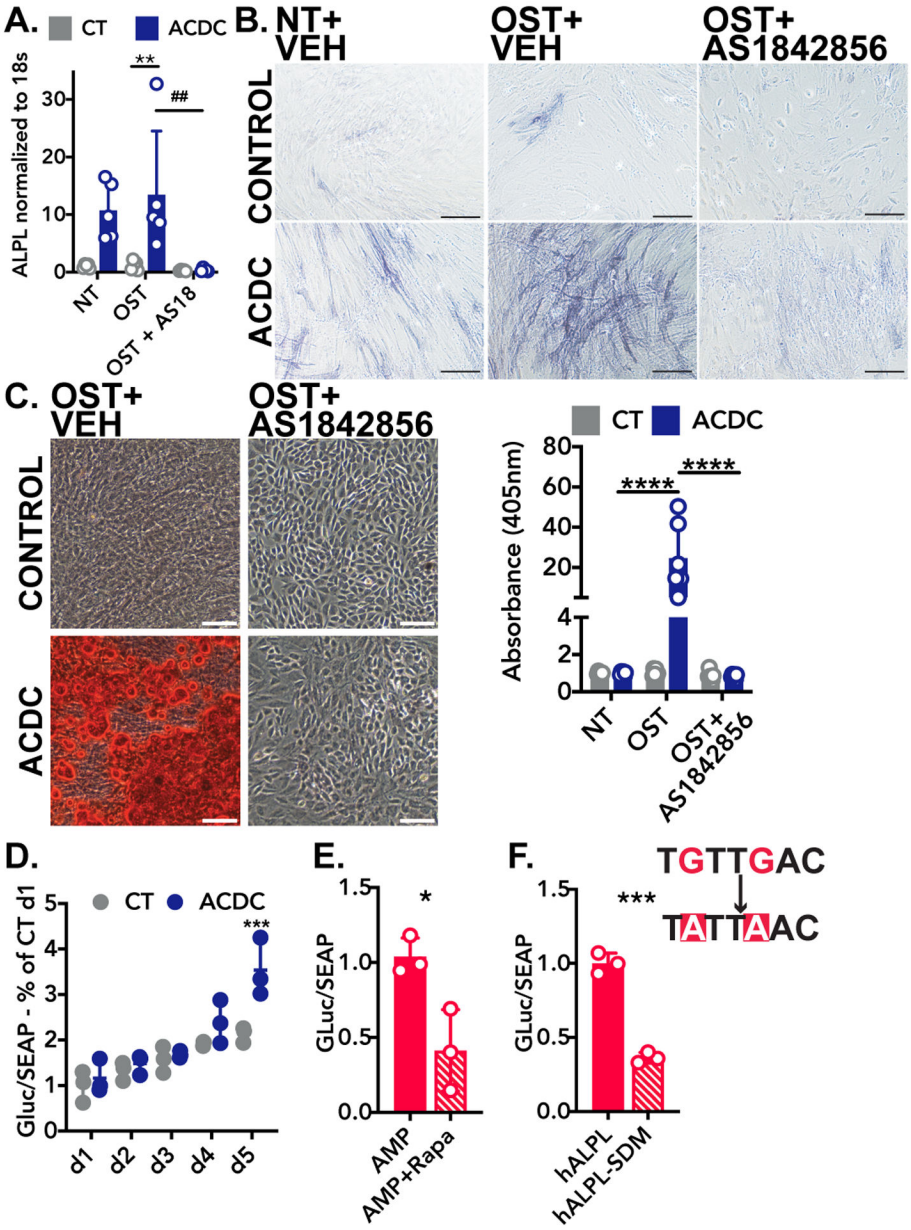

FIGURE 4: FOXO1 inhibitor prevents calcification via reducing *ALPL* promoter activation.

A. RT-qPCR analysis of *ALPL* mRNA isolated from cells in osteogenic conditions receiving 1μM AS-184856 for 5 days. Results representative of n=5 per group using 3 control and 3 ACDC patient cell lines. **p=0.0077, ##p=0.0039. Two-way ANOVA with Tukey's multiple comparison test was used for statistical analysis. **B.** TNAP activity staining in cells cultured for 5 days in osteogenic media supplemented daily with the FOXO1 inhibitor AS-1842856 (1μM) or vehicle control. Results representative of n=5 per group using 4 control and 3 ACDC patient cell lines. Scale bar represents 200um. **C.** Alizarin Red S stain in cells cultured under osteogenic conditions for 21 days and supplemented 1μM AS-1842856. Results representative of n=6 per group using 4 control and 3 ACDC patient cell lines. ****p>0.0001 by two-way ANOVA with Tukey's multiple comparison test. Scale bar

represents 200μm. **D.** Luciferase assay of plasmid DNA containing the Gaussia luciferase under control of the human *ALPL* promoter (hALPL). Cells were transfected with 1μg of plasmid and cultured for 5 days under osteogenic stimulation. Results representative of n=3 per group using 3 control and 3 ACDC patient cell lines. ***p=0.0011 by two-way ANOVA with Sidak's multiple comparisons test. **E.** Luciferase assay of hALPL plasmid in cells treated with 100 μM AMP with and without pretreatment of 200nM rapamycin. Results representative of n=3 using 1 ACDC patient cell line. *p=0.0406. **F.** Luciferase assay of hALPL and Luciferase assay of hALPL with site-directed mutagenesis (SDM) of the putative FOXO1 binding site. Results representative of n=3 using 1 ACDC patient cell line. ***p=0.0008. Unpaired t test with Welch's correction was used for E and F.

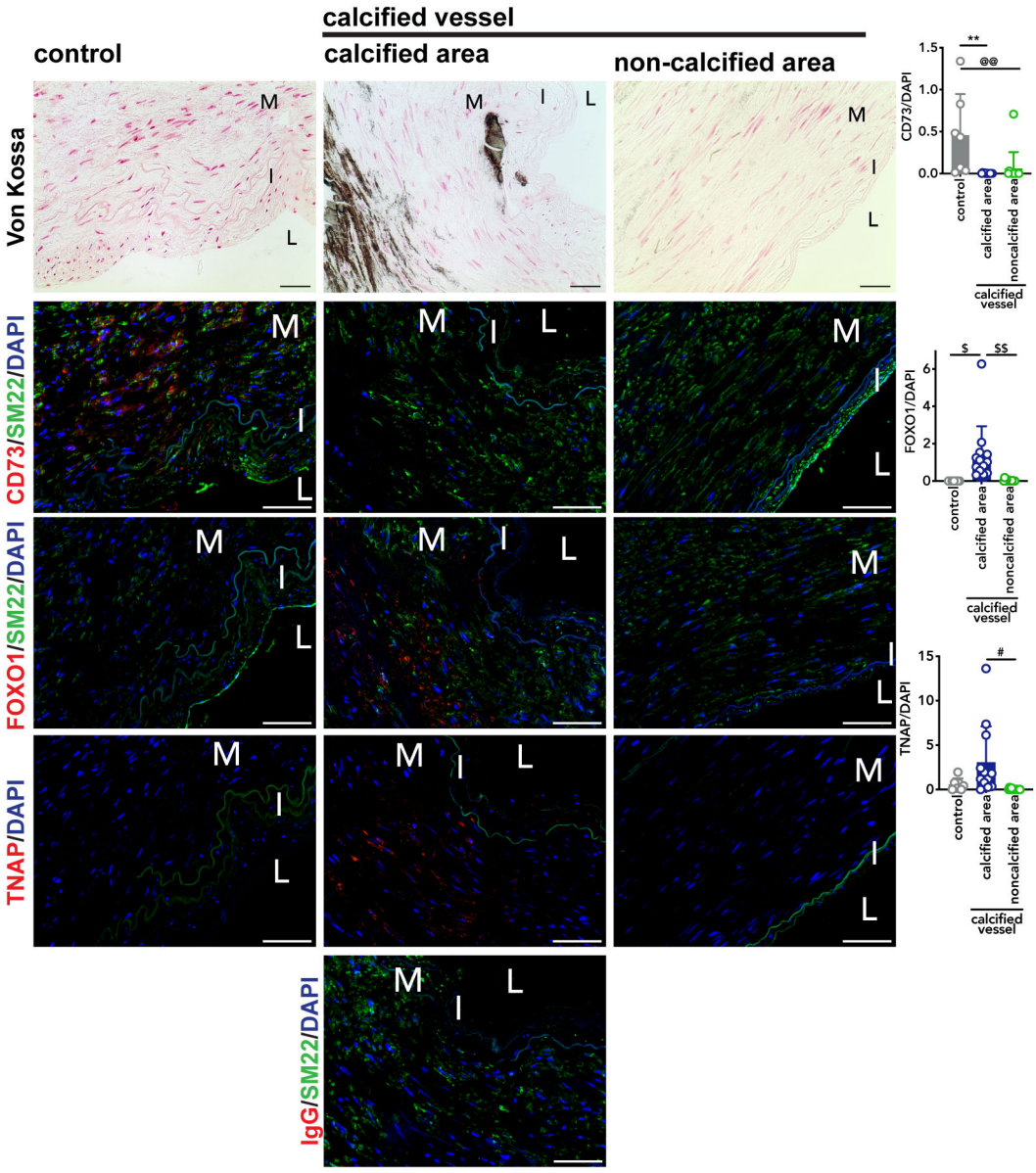

FIGURE 5: CD73 levels reduced in non-ACDC calcified femoropopliteal artery exhibiting higher levels of FOXO1.

Sections of femoropopliteal arteries from 20 different patients were stained with Von Kossa stain to detect calcification. Of the 20 patients, no calcification was detected in 7 vessels and the remaining 13 show calcification. Serial sections were stained with CD73, FOXO1, and TNAP antibody, and an IgG control to match concentration of TNAP at 20μg/mL. Pixel quantification was done using ImageJ and normalized to DAPI. **p=0.0023, $^{@@}$p=0.0067, $^{\$}$p=0.0151, $^{\$\$}$p=0.0043, $^{\#}$p=0.0133. M=tunica media. I=tunica intima. L=lumen. Von Kossa scale bar represents 100μm, fluorescent images scale bar represents 50μm.

TABLE 1:

Baseline characteristics of patients for the isolation of control and ACDC cell lines.

Line	Sex	Age	Disease State	Baseline Characteristics
10	F	24	Control patient	Skin biopsy (right arm)
11	F	66	Control patient	Skin biopsy (right abdomen)
80	M	23	Control patient	Skin biopsy
115	M	32	Control patient	Skin biopsy
20	F	54	ACDC patient	Vascular calcifications in iliac, femoral, and tibial arteries; juxta-articular joint capsule calcifications in fingers, wrists, ankles, feet (ref. 5)
21	F	49	ACDC patient	Vascular calcifications in iliac, femoral, and tibial arteries; periarticular calcifications in shoulders, elbows, hands, hips, knees (ref. 5)
24	M	53	ACDC patient	Vascular calcifications in iliac, femoral, and tibial arteries (ref. 5)
25	M	51	ACDC patient	Vascular calcifications in iliac and femoral arteries (ref. 5)
28	F	44	ACDC patient	Vascular calcifications in femoral, tibial, popliteal, and carotid arteries; calcifications in hands, feet, brain (ref. 12)

TABLE 2:

Putative transcription factor binding sites on the human *ALPL* gene promoter

FOXO1

Nucleotide position frequency

A	C	G	T	Consensus Sequence	Promoter Sequence	basepair matching (%)
1	1	0	205	T	T	99%
13	0	194	0	G	G	94%
0	0	0	207	T	T	100%
0	0	0	207	T	T	100%
0	0	121	86	K	G	58%
198	2	4	3	A	A	96%
2	194	3	8	C	C	94%

	Factor name	Position Order	Position (strand)	Core score	Matrix score	Sequence
1	CPBP	2	10 (+)	1	1	GCCCCag
2	MITF	35	41 (+)	1	1	gtCACATgatc
3	TFE	43	42 (−)	1	1	tcACATGa
4	MITF	44	42 (−)	1	1	tcACATG
5	TCFL4	45	42 (−)	1	1	tcACATGa
6	Spi-B	64	68 (+)	1	1	TTCTCc
7	NFATc2	67	76 (−)	1	1	tGGAAAa
8	NFATc4	68	76 (+)	1	1	tGGAAAat
9	NFATc2	69	77 (+)	1	1	GGAAAa
10	NFATc3	70	77 (+)	1	1	GGAAAa
11	NFATc2	71	77 (+)	1	1	GGAAAa
12	YY1	73	79 (−)	1	1	aaAATGG
13	Elk-1	77	93 (+)	1	1	GGAAGt
14	ipf1	78	98 (−)	1	1	tTAATG
15	BRN1	84	99 (+)	1	1	tAATGCa
16	ZNF35	93	144 (+)	1	1	gGAAGA
17	AP-2 gamma	94	154 (+)	1	1	ttGCCTG
18	ER-alpha	97	159 (+)	1	1	TGACCtg
19	NF1C	100	162 (−)	1	1	cCTGGCt
20	Smad1	103	183 (+)	1	1	ggGCAGACa
21	Smad4	105	185 (−)	1	1	gCAGACa
22	NFATc4	110	191 (−)	1	1	atTTTCCc
23	NFATc2	111	192 (−)	1	1	tTTTCC
24	NFATc3	112	192 (−)	1	1	tTTTCC
25	NFATc2	113	192 (−)	1	1	tTTTCC
26	C-Jun	119	228 (−)	1	1	gAGTCA
27	BEN	121	242 (−)	1	1	tgtCGCTG
28	Spi-B	126	313 (−)	1	1	gAGGAA

29	Spi-B	133	346 (+)	1	1	TTCCCc
30	NF1C	148	390 (−)	1	1	cCTGGCt
31	E2F-6	172	418 (+)	1	1	cGTTTCct
32	Spi-B	174	421 (+)	1	1	TTCCTc
33	Smad2	177	442 (−)	1	1	cTGTCT
34	C-Jun	185	452 (+)	1	1	TGACTc
35	SMAD	195	483 (−)	1	1	atggTGTCT
36	Smad4	199	487 (+)	1	1	tGTCTGc
37	GATA-5	201	494 (−)	1	1	cTGTTAa
38	CPBP	205	502 (−)	1	1	gaGGGGC
39	RORbeta	212	522 (−)	1	1	taGGTCA
40	Nkx2–5	231	526 (+)	1	1	tcAAGTG
41	NKX2B	232	526 (−)	1	1	tcAAGTG
42	ERR1	248	537 (−)	1	1	ggccaAGGTCac
43	ESRRA	266	539 (+)	1	1	ccaAGGTCacc
44	SF-1	269	540 (−)	1	1	CAAGGtca
45	ERR3	270	540 (+)	1	1	cAAGGTca
46	NURR1	273	541 (+)	1	1	aaGGTCAc
47	COUP-TF1	274	541 (−)	1	1	aaGGTCA
48	NR1B1	275	541 (+)	1	1	aaGGTCA
49	RXR-ALPHA	276	541 (+)	1	1	aaGGTCA
50	Smad2	281	572 (−)	1	1	cTGTCT
51	SMAD3	283	572 (−)	1	1	ctGTCTG
52	C-Fos	291	575 (+)	1	1	tcTGACTcaa
53	Fra-1	303	576 (−)	1	1	cTGACTca
54	AP1	309	577 (+)	1	1	TGACTca
55	C-Jun	310	577 (+)	1	1	TGACTc
56	JunB	311	577 (+)	1	1	TGACTcaa
57	MYB	318	580 (+)	1	1	ctcAACTGcc
58	MYB	323	582 (+)	1	1	cAACTGcct
59	Elk-1	326	592 (+)	1	1	GGAAGt
60	CPBP	331	602 (+)	1	1	GCCCCtc
61	CPBP	336	632 (−)	1	1	ctGGGGC
62	E2A	346	657 (+)	1	1	ggaCACCTgcggg
63	HTF4	348	659 (+)	1	1	aCACCTgc
64	E47	349	659 (−)	1	1	acACCTGc
65	HTF4	350	660 (+)	1	1	CACCTgc
66	MRF4	351	660 (+)	1	1	CACCTgc
67	slug	352	660 (+)	1	1	CACCTgcgg
68	CPBP	363	704 (+)	1	1	GCCCCtg
69	Smad2	365	708 (−)	1	1	cTGTCT
70	Kid3	374	718 (−)	1	1	GGTGG
71	NMYC	375	731 (−)	1	1	cAGATG

72	Kid3	381	737 (+)	1	1	CCACC
73	ZXDL	382	750 (−)	1	1	gTCCCCt
74	Spi-B	383	756 (+)	1	1	TTCTGc
75	Spi-B	384	762 (+)	1	1	TTCTTc
76	ZNF35	385	766 (−)	1	1	TCTTGc
77	NF1C	388	775 (+)	1	1	aGCCAGg
78	GKLF	391	779 (−)	1	1	agGGAGG
79	Kid3	412	790 (+)	1	1	CCACG
80	GKLF	430	803 (+)	1	1	agcggggGTGGGg
81	MOVO-B	431	804 (+)	1	1	gcGGGGG
82	CPBP	432	804 (−)	1	1	gcGGGGG
83	Churchill	434	805 (+)	1	1	CGGGGg
84	LKLF	444	807 (+)	1	1	gGGGTGgggg
85	LKLF	445	807 (−)	1	1	gGGGTGggg
86	SALL2	447	808 (+)	1	1	GGGTGgg
87	KLF	448	808 (+)	1	1	GGGTGggg
88	Kid3	450	809 (−)	1	1	GGTGG
89	CPBP	453	810 (−)	1	1	gtGGGGG
90	C-Jun	467	821 (−)	1	1	gAGTCA
91	HIF-1alpha	522	832 (+)	1	1	gCACGT
92	HIF-1alpha	523	832 (+)	1	1	gCACGTgg
93	USF	524	832 (−)	1	1	gcACGTGg
94	Myc	525	832 (−)	1	1	gcACGTG
95	USF2	526	833 (+)	1	1	CACGTg
96	Myc	527	833 (+)	1	1	CACGTgg
97	MAX	528	833 (−)	1	1	CACGTg
98	USF2	529	833 (−)	1	1	cACGTG
99	MAX	531	833 (+)	1	1	cACGTG
100	Kid3	532	835 (−)	1	1	CGTGG
101	Smad2	533	844 (+)	1	1	AGACAg
102	Smad2	537	852 (+)	1	1	AGACAg
103	CLOCK:BMAL	598	860 (+)	1	1	aCACGTgg
104	USF2	600	861 (+)	1	1	CACGTg
105	Myc	601	861 (+)	1	1	CACGTgg
106	MAX	602	861 (−)	1	1	CACGTg
107	USF2	604	861 (−)	1	1	cACGTG
108	MAX	607	861 (+)	1	1	cACGTG

109	HIF2A	609	862 (+)	1	1	ACGTGggc
110	Kid3	610	863 (−)	1	1	CGTGG
111	Smad2	612	882 (+)	1	1	AGACAg
112	NF-1B	619	901 (+)	1	1	GCCAGatat
113	GATA-5	620	903 (−)	1	1	cAGATA
114	**FOXO1**	**624**	**909 (+)**	**1**	**1**	**TGTTGac**
115	MEIS1	627	911 (+)	1	1	tTGACAg
116	Meis2	628	911 (+)	1	1	tTGACAg
117	Smad2	635	924 (+)	1	1	AGACAg
118	PU.1	643	937 (+)	1	1	agaGGAAG
119	Spi-B	644	938 (−)	1	1	gAGGAA
120	Elf-1	645	939 (+)	1	1	AGGAAg
121	PU.1	646	939 (+)	1	1	AGGAAg
122	Smad4	651	945 (−)	1	1	gCAGACa
123	Sox-10	653	948 (−)	1	1	gACAAAg
124	Sox-10	654	949 (−)	1	1	ACAAAg
125	Sox-4	655	949 (−)	1	1	ACAAAga
126	TCF-1	657	949 (−)	1	1	aCAAAG
127	Kid3	660	960 (−)	1	1	GGTGG
128	Sox-10	663	966 (−)	1	1	gACAAAg
129	Sox-10	664	967 (−)	1	1	ACAAAg
130	Sox-4	665	967 (−)	1	1	ACAAAga
131	TCF-1	666	967 (−)	1	1	aCAAAG
132	Kid3	667	977 (+)	1	1	CCACC
133	ING4	668	977 (+)	1	1	cCACCA
134	Spi-B	675	989 (−)	1	1	gCAGAA
135	Elf-1	676	994 (+)	1	1	AGGAAg

136	PU.1	677	994 (+)	1	1	AGGAAg
137	ZNF35	678	995 (+)	1	1	gGAAGA
138	MEL1	679	996 (+)	1	1	GAAGAt
139	ER-alpha	700	1041 (−)	1	1	caGGTCA
140	HNRPUL1	709	1050 (+)	1	1	gCCCAGg
141	PU.1	716	1066 (+)	1	1	agaGGAAG
142	Spi-B	717	1067 (−)	1	1	gAGGAA
143	Elf-1	718	1068 (+)	1	1	AGGAAg
144	PU.1	719	1068 (+)	1	1	AGGAAg
145	ZNF449	724	1074 (−)	1	1	ggcTGGGCtggg
146	TORC2	725	1077 (+)	1	1	TGGGCtggg
147	CPBP	727	1081 (−)	1	1	ctGGGGC
148	Zfp536	738	1091 (+)	1	1	cCGGAGg
149	CPBP	745	1114 (−)	1	1	gcGGGGC
150	SREBP-1	782	1145 (+)	1	1	CACCCca
151	HSF4	807	1172 (−)	1	1	ccGGCAG
152	ZNF300	817	1176 (+)	1	1	cAGGGGgcg
153	CPBP	818	1176 (−)	1	1	caGGGGG
154	Kid3	846	1194 (−)	1	1	CGTGG
155	CPBP	869	1211 (−)	1	1	gcGGGGC
156	ZF5	875	1214 (+)	1	1	GGGCGcgg
157	E2F	878	1215 (+)	1	1	GGCGCg
158	CPBP	884	1218 (−)	1	1	gcGGGGC
159	AP-2alpha	905	1228 (−)	1	1	ggccgGGGGCg
160	CPBP	918	1230 (−)	1	1	ccGGGGG
161	Churchill	928	1231 (+)	1	1	CGGGGg
162	Egr-1	931	1231 (−)	1	1	cggGGGCGg

163	ETF	943	1231 (−)	1	1	cgggGGCGGgg
164	Sp1	955	1232 (−)	1	1	gggGGCGGgg
165	SP4	956	1232 (−)	1	1	gggGGCGGggc
166	SP1	957	1232 (−)	1	1	gggGGCGGggc
167	Sp1	958	1232 (+)	1	1	gggGGCGGggc
168	SP1	963	1232 (−)	1	1	gggggCGGGG
169	BTEB2	965	1233 (+)	1	1	GGGGCggggc
170	BTEB2	967	1233 (−)	1	1	gGGGCGgggc
171	EKLF	969	1233 (+)	1	1	gGGGCGgggccggg
172	Sp2	971	1233 (+)	1	1	gGGGCGggg
173	Sp1	976	1233 (+)	1	1	ggGGCGGggc
174	Sp1	977	1233 (+)	1	1	ggGGCGGggc
175	Sp3	978	1233 (+)	1	1	ggGGCGGggccg
176	E2F-3	986	1235 (+)	1	1	GGCGGgg
177	CPBP	987	1236 (−)	1	1	gcGGGGC
178	ZAC	990	1238 (+)	1	1	gGGGCCg
179	CPBP	993	1242 (−)	1	1	ccGGGGC
180	ZAC	995	1244 (+)	1	1	gGGGCCg
181	MZF-1	1004	1254 (+)	1	1	tGGGGAg
182	MAZ	1007	1255 (+)	1	1	gGGGAGgg
183	CKROX	1012	1255 (−)	1	1	gggGAGGGg
184	ZAC	1027	1266 (+)	1	1	gGGGCCg
185	AP-2alpha	1045	1268 (−)	1	1	ggccgGGGGCg
186	CPBP	1057	1270 (−)	1	1	ccGGGGG
187	Churchill	1068	1271 (+)	1	1	CGGGGg
188	Egr-1	1071	1271 (−)	1	1	cggGGGCGg
189	ETF	1079	1271 (−)	1	1	cgggGGCGGgg

190	Sp1	1090	1272 (−)	1	1	gggGGCGGgg
191	SP1	1097	1272 (−)	1	1	gggggCGGGG
192	Sp2	1104	1273 (+)	1	1	gGGGCGggg
193	E2F-3	1122	1275 (+)	1	1	GGCGGgg
194	MOVO-B	1126	1276 (+)	1	1	gcGGGGG
195	CPBP	1127	1276 (−)	1	1	gcGGGGG
196	ZBP89	1128	1276 (−)	1	1	gcGGGGGagggg
197	Churchill	1134	1277 (+)	1	1	CGGGGg
198	WT1	1144	1278 (−)	1	1	gggGGAGGg
199	MAZ	1154	1279 (+)	1	1	gGGGAGgg
200	CKROX	1155	1279 (−)	1	1	gggGAGGGg
201	MAZ	1162	1280 (+)	1	1	gGGAGGggg
202	SP1:SP3	1168	1281 (−)	1	1	ggaGGGGGcgg
203	CPBP	1175	1282 (−)	1	1	gaGGGGG
204	NF-E4	1198	1301 (−)	1	1	gCCTCAc
205	CPBP	1208	1312 (+)	1	1	GCCCCgc
206	CDX-2	1212	1326 (+)	1	1	TTTATa
207	ETF	1219	1334 (+)	1	1	gcGGCGG
208	E2F-3	1222	1336 (+)	1	1	GGCGGgg
209	MOVO-B	1227	1337 (+)	1	1	gcGGGGG
210	CPBP	1228	1337 (−)	1	1	gcGGGGG
211	Churchill	1230	1338 (+)	1	1	CGGGGg
212	LKLF	1238	1340 (+)	1	1	gGGGTGgtgg
213	Kid3	1242	1342 (−)	1	1	GGTGG
214	ING4	1243	1344 (−)	1	1	TGGTGg
215	Kid3	1244	1345 (−)	1	1	GGTGG
216	ZF5	1275	1377 (−)	1	1	ccgCGCCC

217	E2F	1276	1378 (−)	1	1	cGCGCC
218	NF1C	1283	1390 (−)	1	1	cCTGGCt
219	Kid3	1303	1405 (+)	1	1	CCACG
220	HES-1	1306	1411 (+)	1	1	gcTTGTGc
221	CPBP	1323	1466 (+)	1	1	GCCCCgc
222	ZF5	1328	1469 (−)	1	1	ccgCGCCC
223	E2F	1330	1470 (−)	1	1	cGCGCC
224	Spi-B	1335	1480 (+)	1	1	TTCCCc
225	CPBP	1341	1489 (+)	1	1	GCCCCag
226	Kid3	1349	1500 (−)	1	1	CGTGG
227	Spi-B	1354	1514 (+)	1	1	TTCTGc
	TSS	1354				

TABLE 3:

Patient characteristics of popliteal artery samples

Femoropopliteal Artery Patient Information												
NORS #	**Sex**	**Age**	**Disease State (transverse)**	**Disease State (longitudinal)**	**Cause of Death**	**Body Mass Index**	**Hyper-tension**	**Diabetes**	**Dyslipidemia**	**Coronary Artery Disease**	**Pack-year smoking**	**Alcohol abuse**
VON KOSSA POSITIVE												
N 372	M	27	4	2.7	Cardiac arrest	27.3	No	No	No	No	No	No
N 178	F	39	5	5	Cardiac arrest	47.3	No	Yes, since 7 yo		No	No	No
N 429	M	39	4	4	Cardiac arrest	31.1	No	No	No	No	3	No
N 403	M	43	5	4	Cardiac arrest	22.7	No	No	No	No	No	No
N 62	M	48	6	6	ICH/Stroke	25.6	Yes, since 42 yo	Yes, since 14yo	No	No	32	Yes, 12 drinks/day for last 23 years
N 319	M	80	5	6	Respiratory failure	31.4	Yes, since 74 yo	Yes, since 78 yo	No	No	66	Yes, 16 drinks/day as adult
N 159	M	77	6	5	Multi system failure	29	Yes, unknown timeframe	Yes, since 53 yo	Yes, unknown timeframe	No	2	No
N 269	M	70	5	5	Cardiac arrest	27.1	No	No	No	No	No	No
N 60	M	70	4	5	Cardiac arrest	30.2	Yes, since 55 yo	Yes, since 60 yo	Unsure	Yes	No	No
N 431	M	69	6	5.3	Cardiac arrest	26.3	Yes, since 46 yo	Yes, since 46 yo	Yes, since 46 yo	No	25	No
N 317	M	48	3	2.7	Cardiac arrest	28.3	Yes	Yes, since 41 yo	No	Yes	No	No
N 316	M	82	3	3	N/A	N/A	N/A	N/A	N/A	N/A	N/A	N/A
N 213	M	78	3	2.5	Myocardial infarction	25.4	Yes, since 39 yo	No	No	Yes	15	Yes
VON KOSSA NEGATIVE												
N 177	M	27	1	1	Cardiac arrest secondary smoke inhalation	34.3	No	No	No	No	13	0
N 126	F	39	1	1	Cardiac arrest	43.5	Yes	No	Yes	No	No	No
N 201	M	39	2	2	Suicide	33.1	Yes	No	No	No	16	No
N 36	F	43	1	1	Cardiac arrest	36.7	No	No	No	No	9.5	Yes, 6 drinks / weekends for past 15 yrs
N 136	M	71	2	2.7	Cardiac arrest	28.3	Yes	No	Yes	No	45	No
N 413	M	68	4	2.7	Cardiopulmonary arrest	25.2	Yes, since 67 yo	No	No	No	20	Yes, 5–6 drinks/day for 40 years. Quit 10–

Femoropopliteal Artery Patient Information													
NORS #	**Sex**	**Age**	**Disease State (transverse)**	**Disease State (longitudinal)**	**Cause of Death**	**Body Mass Index**	**Hyper-tension**	**Diabetes**	**Dyslipidemia**	**Coronary Artery Disease**	**Pack-year smoking**	**Alcohol abuse**	
												12 years ago.	
N 329	M	68	4	3.3	Cardiac arrest	38.6	Yes, since 48 yo	No	Yes, 20+ years	No	No	No	

Disease State was determined using Van Gieson's stained sections and graded on a scale from 1 (no disease) to 6 (severe disease) as per PMID: 29371245 and PMID: 26766633.

Grading was done using both conventional transverse and longitudinal sections of the artery. In the longitudinal direction used 3 sections per subject and averaged the results.